Ceramics International **24** (1998) 45–51

PII: S0272-8842(96)00076-4
0272-8842/97 $17.00+.00

Microstructural Design and Mechanical Properties of a Ternary Partially Stabilised Zirconia Alloy

R. H. J. Hannink,[a]* V. Gross[a] & B. C. Muddle[b]

[a]CSIRO, Division of Materials Science and Technology, Normanby Road, Clayton, Victoria 3168, Australia
[b]Department of Materials Engineering, Monash University, Wellington Road, Clayton, Victoria 3168, Australia

(Received 17 April 1996; accepted 29 August 1996)

Abstract: The transformation toughening mechanism in zirconia-toughened ceramics is temperature limited. An attempt has been made to design a ternary partially stabilised zirconia alloy, based on CeO_2–MgO–ZrO_2, in which the transformation toughening component of the measured mechanical properties is retained at low to intermediate temperatures, while other mechanisms for improving strength and toughness are invoked and become dominant at high temperatures. Mechanical property results indicate that the microstructures developed, which contain elongated, dispersed tetragonal zirconia particles, may produce useful toughening enhancement. However, the material fabrication route used requires refinement. © 1997 Elsevier Science Limited and Techna S.r.l.

1 INTRODUCTION

Zirconia-based ceramic alloys are well known for their potential for transformation toughening, which provides the capability for combining high strength and toughness through the careful control of alloying additions and thermal treatment.[1–4] However, transformation toughening is associated with a stress-activated tetragonal to monoclinic transformation in tetragonal zirconia and can generally not be invoked at temperatures above about 300°C, due mainly to the thermodynamic stability of the tetragonal phase as temperature is increased.[5]

A number of other ceramic systems have been examined as potential sources of high temperature transformation toughening;[6] however, none appears feasible or has been developed commercially. Nevertheless, it is desirable for ceramic systems to have improved toughness beyond the range of transformation toughening and the present research program has involved examination of how a range of alternative toughening mechanisms[7–12] might be activated in a transformation-toughened partially-stabilised zirconia alloy solely through the manipulation of the microstructure by control of composition and post-sintering heat treatments. The present paper reviews recent efforts to model precipitate forms and optimise microstructural development in a $Ce0_2$/MgO–PSZ ternary alloy, and attempts to correlate measurements of mechanical properties with semi-quantitative characterisation of microstructure in the alloy.

2 BACKGROUND

Two general forms of toughening mechanism have been identified for engineering ceramics.[7] These have been termed intrinsic and extrinsic, and they are distinguished in the method by which propagating cracks interact with the inherent microstructure. Extrinsic mechanisms are by far the most common and arise from the microstructural features which shield the crack from the applied stress.

For crack-shielding toughening mechanisms, it is commonly assumed that the fracture toughness,

*To whom correspondence should be addressed.

K_{1c}, of a ceramic is determined by the sum of the various individual contributions to toughness. While this is an obvious over-simplification, it does give an indication of the possible toughness achievable. Thus, for the systems to be considered here, the toughness may take the form:

$$K_{1c} = K_m + \Delta K_i$$
$$\Delta K_i = \Delta K_T + \Delta K_{mc} + \Delta K_{cb} + \Delta K_s + \Delta K_{cd} \quad (1)$$

where K_{1c} is the measured toughness of the system, K_m the matrix toughness and the ΔK_i represent the incremental contributions from transformation toughening (ΔK_T), micro-cracking (ΔK_{mc}), crack bridging (ΔK_{cb}), frictional sliding (ΔK_s) and crack deflection or meandering (ΔK_{cd}), respectively. The contributions from the various mechanisms have been reviewed in detail elsewhere.[8] We shall briefly outline the significant microstructural features required in each case for potentially enhanced toughening.

Transformation toughening[4] is derived from the dilational and shear strains associated with the tetragonal to monoclinic phase transformation in zirconia. These strains reduce the crack-tip stresses through the formation of a zone of transformation behind and in front of the crack tip. The contribution to toughness attainable through the stress-activated transformation[2,4] is controlled by the effective modulus of the ceramic, the dilational strain associated with the tetragonal to monoclinic transformation of particles and precipitates, the volume fraction of transformed particles in the process zone adjacent to the crack, V_f, and the transformation or process zone height or width, h. For MgO–PSZ ceramics, the general approach to maximising the transformation toughening increment has been to set V_f at about 40% and the precipitate size at $\sim 0{\cdot}2\,\mu$m, so that transformation can be stress-induced at room temperature and the dimensions of the process zone are thus maximised.[4]

The micro-crack toughening increment may be viewed as arising from an increase in the fracture surface in the material adjacent to, but not in front of, the crack tip. Micro-crack toughening, being reasonably temperature-insensitive, holds considerable promise as a high-temperature toughening process.[11] The potential contribution to toughness is determined by the effective modulus of the matrix (E^*), the Poisson's ratio of the material, the volume fraction of particles which may be associated with micro-cracks and the process zone height.

Crack bridging operates during the propagation of the crack when microstructural features such as fibres, precipitates or individual grains bridge the separating surfaces behind the crack front. The mechanism relies on residual thermal expansion anisotropy stresses to suppress intergranular fracture, hence leaving an intact bridge in the crack's wake. Crack bridging is another mechanism which could be operative at elevated temperatures for tetragonal precipitates in a cubic matrix, if the precipitates were of a scale capable of effectively spanning a propagating crack.

Frictional sliding becomes operative when crack bridges fail by surface debonding and the surfaces commence to slide over each other. As the bridge commences to fail, a toughening increment arises due to the occurrence of frictional sliding losses.

Crack meandering and deflection can occur when a crack is deflected or caused to deviate from the maximum tensile stress axis, with the effect that the local crack tip stress will be reduced. An additional toughening increment is thus possible if a matrix contains particles which can influence the direction of a propagating crack. Faber and Evans[12] have calculated toughening increments for rod-shaped inclusions of various aspect ratios, and found that the composite toughness may be as high as 1·5 times that of inclusion-free matrix when the aspect ratio of the inclusions approaches a value of 12:1. The toughening increment is dependent upon the aspect ratio, but is relatively insensitive to inclusion size.

For MgO–PSZ systems, where the precipitates take on a lenticular morphology,[4,15] all five toughening mechanisms may contribute to the fracture resistance of the material, with their contributions dependent primarily on volume fraction of precipitates, process zone width and temperature. The present research has been aimed at exploiting the various toughening mechanism in MgO–PSZ based materials, such that transformation toughening operates at low temperatures, while the potential high temperature toughening processes based on micro-cracking, crack bridging, wedging, deflection, meandering and particle pull-out may become operative at high temperatures.

Selection of a suitable material was made on the premise that the precipitates in the zirconia alloy should remain in the tetragonal form, while also retaining the disc morphology characteristic of MgO–PSZ, preferably with an increase in aspect ratio during the growth process.[13,14] These specifications should produce maximum benefit of the possible toughening mechanisms described previously. Thus the alloy requires two forms of stabiliser, one with a high solubility and one with a low solubility in the zirconia matrix at low temperatures. To satisfy these criteria CeO_2 and

MgO were selected as the high and low solubility stabilisers, respectively.

To assist in alloy design, preliminary calculations were made of tetragonal (t) precipitate morphology and crystallography using the approach of Khachaturyan.[16] The results of this modelling, which have been presented elsewhere,[13,14] indicated that the habit plane of the tetragonal particles in CeO_2–MgO–ZrO_2 alloy would remain within $\pm 10°$ of the $\{001\}_c$ habit observed in binary MgO–PSZ alloys. They also suggested that the aspect ratio of the particles should increase if the misfit between tetragonal and cubic phases were decreased. This led to the selection of alloy compositions which would exhibit a reduction in the lattice misfit defined by the parameter $t=(a_t-a_c)/(c_t-a_c)$, where a_c and a_t, and c_t are the lattice parameters of the cubic and tetragonal phases, respectively. As an example, a 1·25 mol% CeO_2–10·8 mol% MgO alloy was found to have lattice parameters of:

$$a_c = 0 \cdot 5093 \text{ nm and } a_t = 0 \cdot 5091 \text{ nm}, \; c_t = 0 \cdot 5184 \text{ nm},$$

and a value of $t=-0{\cdot}022$, compared to a value of $t=-0{\cdot}028$, for binary 9·4 mol% MgO–PSZ.[15] This small decrease in t was sufficient to ensure a significant increase in aspect ratio for equivalent heat treatment conditions.

3 EXPERIMENTAL PROCEDURES

Based on the outcome of modelling studies,[13,14] for which the alloys selected should retain a plate-like lenticular shape while coarsening, the two alloy compositions selected were 1·25 and 2·5 mol% CeO_2 with 10·8 mol% MgO, 0·25 mol% SrO and the remainder ZrO_2. These two alloys are hereinafter referred to as 1·25 and 2·5 Ce/Mg–PSZ, respectively. For the aspect ratio studies, a control MgO–PSZ alloy, containing 10·8 mol% MgO, was also used and given the same thermal treatments.

The green compacts were fabricated by conventional powder processing techniques, which included heating in a controlled manner to 1700°C, holding for 2 h, cooling at 500°C·h^{-1} to 1000°C and thereafter furnace cooling to room temperature. Ageing was conducted in an electrically-heated furnace for various times at 1400°C.

Microstructural characterisation was carried out using optical, scanning (SEM) and transmission (TEM) electron microscopy. Optical and SEM surfaces were prepared by diamond polishing to a 1 μm finish and etching for 3·5 min. in HF. Precipitate aspect ratios were determined from TEM micrographs obtained near $<001>_c$ orientations; the apparent thickness and length were measured for a minimum of 100 well-defined particles.

The fraction of transformable tetragonal phase was estimated from the difference between the ground and polished surface phase contents as determined by the ratio of the areas under the {111} cubic/tetragonal and monoclinic phase X-ray diffraction peaks.[17]

Flexural bend strength was measured using the four-point load configuration, by crack initiation from the polished face of a 3×3×40 mm test bar using a centre span of 12 mm. High temperature mechanical properties were determined in three-point flexure using specimens of similar dimensions at temperatures of 1000 and 1150°C. Fracture toughness was ascertained using the Evans and Charles indentation approach.[18]

4 RESULTS AND DISCUSSION

4.1 Changes in precipitate growth

Isothermal ageing of the Ce/Mg–PSZ alloys for up to 32 h at 1400°C produced lenticular precipitate plates of average diameter up to 0·5 μm, with an aspect ratio of ~9:1, although aspect ratios as large as 16:1 were observed. Details of the precipitate development, size, aspect ratio and grain size as a function of composition and ageing time at 1400°C have been reported elsewhere[14] and only a brief description is warranted here.

The sample aged for 2 h contained precipitates of a similar size and morphology to those typically observed for a 9·4 mol% MgO–PSZ alloy,[15] 2 h being about the optimal ageing time for this Mg–PSZ alloy at 1400°C. The 16 h-aged sample achieved an aspect ratio of 8·2:1 and a size of approximately 0·5 μm; at this scale and aspect ratio the precipites in the 1·25 Ce/Mg–PSZ sample aged for 16 h show considerable promise of approaching the morphology required for high-temperature toughening mechanisms.

Since the transformation toughening mechanism is inoperative at high temperatures,[5] an attempt has been made to optimise the other mechanisms by microstructural manipulation of the precipitate morphology. Using established equations developed by various workers,[9–12] it is possible to estimate the toughening contributions achievable from the precipitate morphology developed to date. We will now discuss briefly the potential partial contribution of these other mechanisms as a function of precipitate morphology.

It has been shown that both micro-cracking and grain bridging mechanisms of toughening are

independent of precipitate shape;[4] only grain or particle volume needs to be considered, for its role in determining the magnitude of thermal expansion and transformation dilation misfits. For micro-cracking, a larger precipitate volume would produce a greater propensity to induce micro-cracks associated with crack propagation. Due to their higher localised lattice strains, the presence of larger precipitates is an obvious advantage.

The potential toughness contribution due to grain bridging is dependent upon the scale of linkages across the fracture surfaces and the larger t particles in the present alloys would be expected to lead to a slightly greater increment to toughening than those of conventional Mg–PSZ. However, this toughening increment would be expected to decrease with increasing temperature due to the smaller temperature difference between the testing and ageing temperatures; the greater thermal expansion of the tetragonal c-axis[4] results in increased matrix constraint on the precipitate and a reduction to the toughening contribution.

The frictional sliding mechanism is temperature independent and thus should be an advantage for high-temperature toughness.[11] The large precipitate sizes and increased aspect ratios generated in the Ce/Mg–PSZ alloys may be estimated, from Ref. 9, to yield a toughening increment of about three times that of MgO–PSZ. The larger precipitate size and increased aspect ratio of the particles in the ternary alloy present a larger surface area of interphase boundary over which this mechanism operates.

The final mechanism to consider is that of crack deflection and meandering. Using data given by Faber and Evans,[12] an increased precipitate aspect ratio is expected to provide increased crack deflection and thus an increase in fracture energy. For this mechanism, however, larger precipitate size alone is of little value and aspect ratio is the important parameter.

4.2 Mechanical property measurements

The strengths of the aged 1·25 Ce/Mg–PSZ samples, as measured in four-point flexure, are shown in Fig. 1 as a function of ageing condition. The bend strength data of a transformation-toughened 9·4 mol% MgO–PSZ material, also aged at 1400°C (CSIRO, unpublished data), is included for comparison. From the data in Fig. 1, it is evident that the ternary alloy also responds to ageing treatment and the trend in strength with time indicates the main toughening mechanism is attributable to stress-induced transformation. This can be inferred from the observation that the strength deteriorates at ageing times beyond 16 h, which is consistent

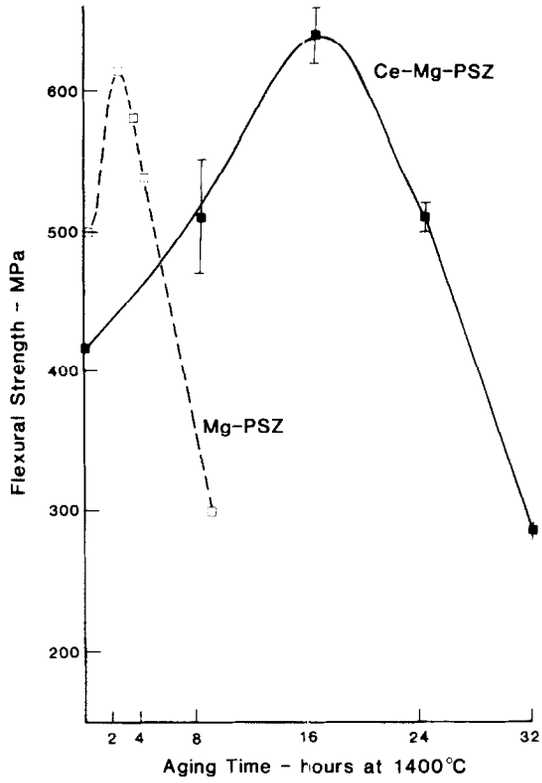

Fig. 1. Room temperature flexural bend strength of the 1.25 Ce/Mg–PSZ alloy aged for various times at 1400°C. Also shown for comparison is the strength of a 9.4 mol% Mg–PSZ alloy, also aged for various times at 1400°C.

with the development of a microstructure that is over-aged. The maximum strength attained is, within experimental error, the same as that for the comparable MgO–PSZ alloy.

The room temperature indentation fracture toughness[18] values were determined as 3·4, 3·9, 5·1 and 3·5 MPa·m$^{1/2}$, for the as-fired and 8, 16 and 32 h-aged samples, respectively. The fracture toughness trend is similar to that for 1400°C aged Mg–PSZ materials,[4] which also shows a peak toughness and strength with ageing time. Relative fracture toughness values between this and other systems cannot be compared due to the variety of techniques used.

Figure 2 shows the flexural strength data for the 1·25 Ce/Mg–PSZ alloy measured at 1000 and 1100°C. With the exception of the as-fired material tested at 1000°C, the strength was independent of ageng time within experimental error. This result was somewhat unexpected in that variations in the intragranular microstructure would be expected to influence the propagating crack through crack-shielding mechanisms.

4.3 Microstructural characterisation

Assuming that the 1·25 mol% CeO_2 addition has very little effect on the position of the phase

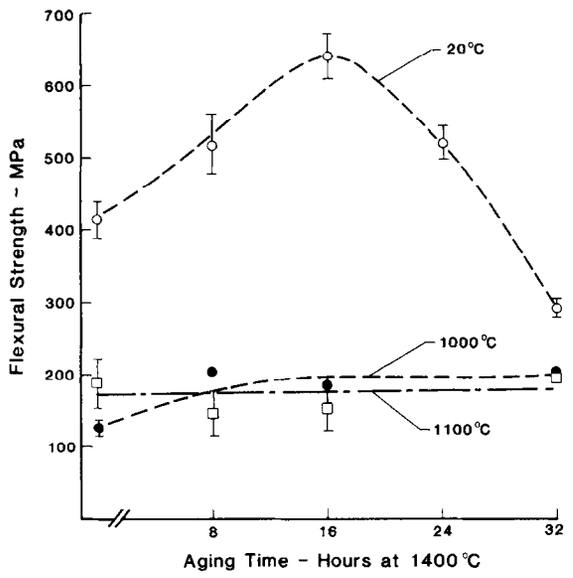

Fig. 2. Room temperature, 1000 and 1100°C bend strength of 1.25 Ce/Mg–PSZ as a function of ageing time at 1400°C.

boundary at 1400°C, the equilibrium tetragonal phase content at 1400°C was estimated from the ZrO_2–MgO phase diagram[19] to be approximately 27 vol.%, compared to 37 vol.% for a conventional 9·4 mol% MgO–PSZ alloy. These phase content figures reflect the total fraction of t-phase which might become available for transformation toughening. In practice, approximately 70% of the t-phase might be expected to contribute in optimally aged materials.

To determine the fraction of transformable tetragonal (tt) phase, X-ray diffraction data was collected from both polished and diamond ground surfaces to assess the tetragonal phase content. The difference between the two measured values indicates the amount of tt. The results for the as-fired, 8 h, 16 h and 32 h-aged samples were 4, 15, 7 and 0% tt, respectively.

Optical microscopy and SEM were used to examine the microstructural features which might account for the mechanical property behaviour. Polished and etched surfaces revealed that the average grain diameters for all the bend strength samples were in the range 20–40 μm and that the porosity, at approximately 5%, was uniformly distributed. The average pore size was typically $\sim 2\,\mu$m, with individual pores up to 5 μm in scale.

Scanning electron microscopy was carried out on the polished and etched surfaces and the fracture surfaces. Figure 3(a)–(c) illustrates the variation in precipitate size and morphology for the 8, 16 and 32 h-aged samples. The main features of these micrographs include the interaction between the tetragonal particles to form near continuous lamellae and the deviation from disc-like morphology as the ageing time increases. Another feature of the microstructure was the development of grain boundary regions containing large eutectoid colonies consisting of tetragonal/monoclinic phase in a cubic matrix. The morphology of these regions suggests coarsening of the microstructure as a result of partitioning of the stabilisers. This feature effectively results in large precipitate free zones (PFZs) adjacent to the grain boundaries. Such PFZs would be expected to reduce the toughness of the material, due to the lack of precipitate–crack interaction when the crack propagates across grain boundaries and through the PFZ regions (see, for example, the arrowed region in Fig. 4). The situation would be exacerbated by the small grain size

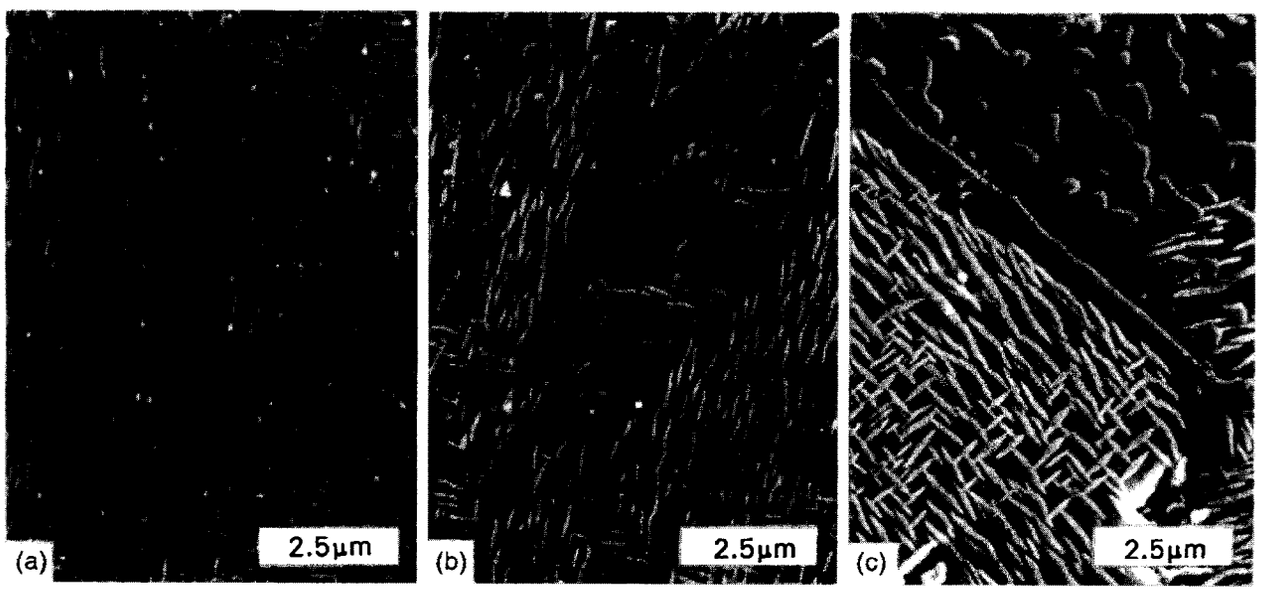

Fig. 3. SEM micrographs illustrating variations in precipitate size and morphology in 1.25 Ce/Mg–PSZ for samples aged at 1400°C for (a) 8 h, (b) 16 h and (c) 32 h. Note the "precipitate free zones" (PFZ) near the grain boundaries in (c) and the irregular nature of the plate face of the precipitates, the $[001]_t$ face, in (a)–(c).

which would lead to a predominantly intergranular fracture mode.

Fractography of the room temperature fracture surfaces indicated significant crack–precipitate interaction, but also evidence of a predominantly intergranular fracture mode and preferred cracking through PFZs. Figure 4 illustrates the crack–precipitate and PFZ fracture mode for the 16 h sample. The fracture surface suggests some evidence of crack meandering and particle pull-out that may contribute to increased toughness, while the cleavage-like nature of cracking through the PFZ regions (arrowed) would be expected to detract from the measured toughness.

Fractography of the three-point flexure samples tested at 1000°C revealed a preponderance of intergranular fracture and massive pore concentrations on the grain facets (see Fig. 5). This fracture behaviour could account for the consistency in the high-temperature fracture properties, in that the propagating crack did not in general interact with the grain–matrix microstructure. In the few cases where intragranular fracture was observed, significant crack–precipitate interaction occurred. Figure 6(a) and (b) highlights this interaction in the 16 h and 32 h samples. It is strongly suggested in these micrographs that the precipitate rafting, or clustering of similar variants, has a considerable influence on the crack propagation. The fracture surface of the 32 h sample is not too dissimilar in appearance to that observed for woven-laminate materials.

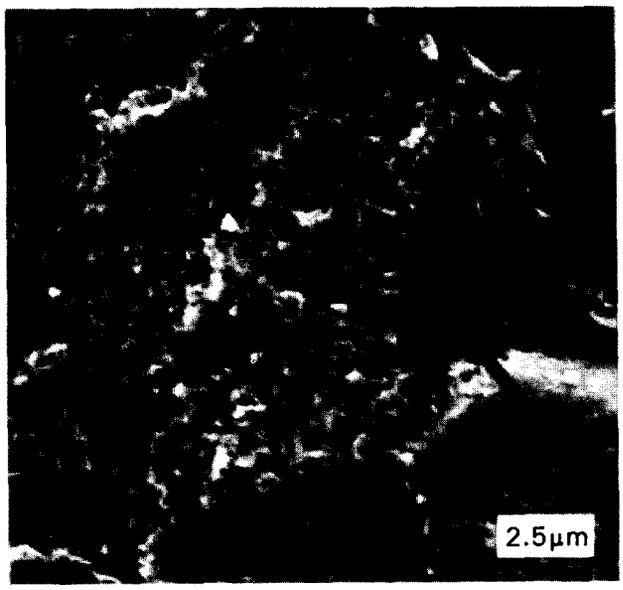

Fig. 4. Room temperature fracture surface of the 16 h-aged sample. Note PFZ interaction (arrowed).

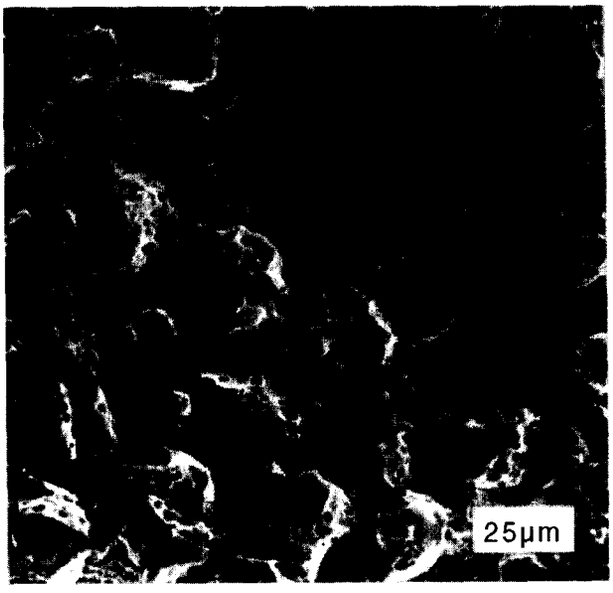

Fig. 5. Fracture surface of 16 h-aged sample tested at 1000°C. Note the preponderance of intergranular fracture.

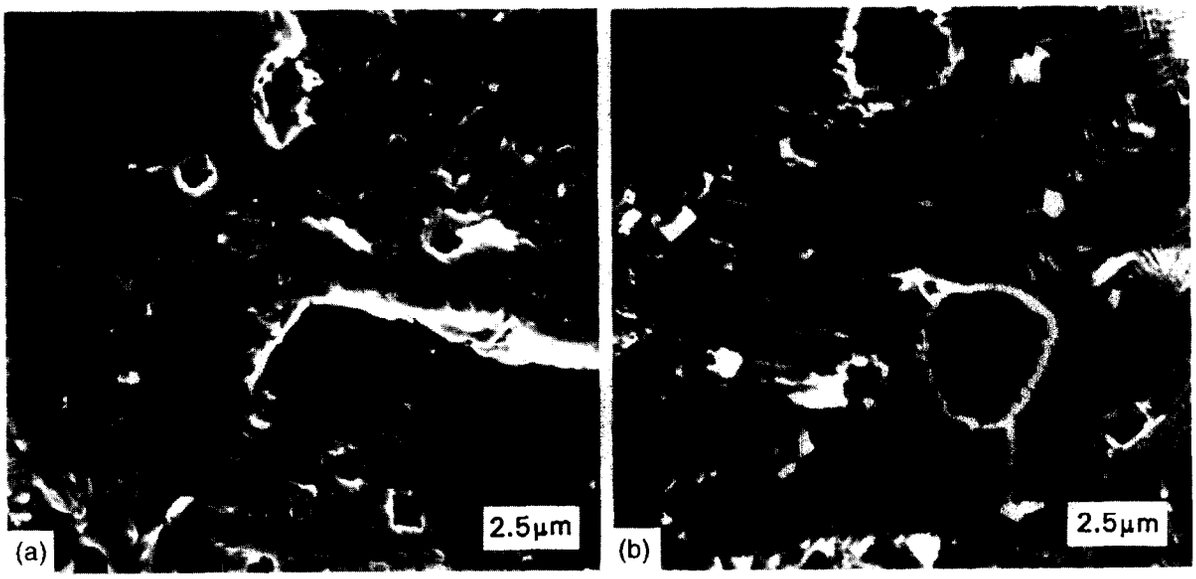

Fig. 6. Fracture surfaces of samples tested at 1100°C showing crack–precipitate interaction for (a) 16 h and (b) 32 h-aged materials.

5 CONCLUSIONS

An attempt has been made to develop, with the assistance of microstructural modelling, a transformation-toughening, zirconia-based ternary alloy which would have the capability of utilising other crack-shielding toughening mechanisms at elevated temperatures. Based on the work to date the following conclusions can be made:

(a) A zirconia-based ternary alloy with 1·25 mol% CeO_2 and 10·8 mol% MgO additions has potential to yield improved microstructural features which permit crack-shielding mechanisms, in addition to transformation toughening, to be utilised.

(b) Based on the microstructures developed, the most promising shielding mechanisms for high-temperature toughness appear likely to be frictional sliding, crack deflection and crack meandering.

(c) The strength and toughness achieved in the 1·25 mol%CeO_2–10·8 mol% MgO–PSZ alloy confirm a significant transformation toughening increment, with potential contributions from the other toughening mechanisms yet to be determined quantitatively.

(d) Improved processing to reduce porosity and additional high-temperature testing are required to fully evaluate the possible contributions from the various crack-shielding mechanisms.

ACKNOWLEDGEMENT

We thank Dr S. Lathabai for assistance with the indentation fracture toughness determinations.

REFERENCES

1. *Science and Technology of Zirconia I–IV*, ed. various. The American Ceramic Society, Columbus, OH, 1981, 1983 and 1988.
2. EVANS, A. G. & CANNON, R. M., *Acta Metall.*, **34** (1986) 761.
3. *Science and Technology of Zirconia V*, ed. S. P. S. Badwal, M. J. Bannister & R. H. J. Hannink. Technomic, Lancaster, PA, 1993.
4. GREEN D. J., HANNINK, R. H. J. & SWAIN, M. V., *Transformation Toughening of Ceramics*. CRC Press, Boca Raton, FL, 1989.
5. BECHER, P. F., SWAIN, M. V. & FERBER, M. K., *Mater. Sci.*, **22** (1987) 76.
6. KRIVEN, W. M., Displacive transformation mechanisms in zirconia ceramics and other non-metals. In *Tailoring Multiphase and Composite Ceramics*. Plenum, New York, 1985, pp. 223–237.
7. RITCHIE, R. O., *Mater. Sci. Eng.*, **A103** (1988) 15.
8. HANNINK, R. H. J. & SWAIN, M. V., *Ann. Rev. Mater. Sci.*, **24** (1994) 359–408.
9. MARSHALL, D. B., DRORY, M. D. & EVANS, A. G., *Fracture Mechanics of Ceramics*, Vol. 6, ed. Bradt, Evans, Lange & Hasselman. Plenum Press, New York, 1983, pp. 289–307.
10. McMeeking, R. & EVANS, A. G., *J. Am. Ceram. Soc.*, **65** (1982) 242.
11. EVANS, A. G., *J. Am. Ceram. Soc.*, **73** (1990) 187.
12. FABER, K. T. & EVANS, A. G., *Acta Metall.*, **31** (1983) 565–577.
13. JENSEN, D. G., HANNINK, R. H. J. & MUDDLE, B. C., *Trans. Mater. Res. Soc. Jpn*, **14A** (1994) 455–458.
14. HANNINK, R. H. J., GROSS, V., JENSEN, D. G. & MUDDLE, B. C., *8th CIMTEC, Vol. C: Ceramics Charting the Future, Paper B11:L12*, Techna S.r.l, Florence, Italy, 1995.
15. HANNINK, R. H. J., *J. Mater. Sci.*, **13** (1978) 2487.
16. KHACHATURYAN, A. G., *Theory of Structural Transformations in Solids*. Wiley, New York, 1983.
17. GARVIE, R. G. & NICHOLSON, P. S., *J. Am. Ceram. Soc.*, **55** (1972) 303.
18. EVANS, A. G. & CHARLES, E. A., *J. Am. Ceram. Soc.*, **59** (1976) 371.
19. GRAIN, C. F., *J. Am. Ceram. Soc.*, **50** (1967) 288.